

DDA , D^*D^*A and D^*DA vertices in the light-cone QCD and considering $B^0 \rightarrow K_1^+ \pi^-$ branching ratio

S. Momeni ^{*}, R. Khosravi [†]

Department of Physics, Isfahan University of Technology, Isfahan 84156-83111, Iran

We investigate the strong coupling constants of DDA , D^*D^*A and D^*DA vertices in the framework of the light-cone QCD sum rules, where A is an axial vector meson such as $a_1, b_1, K_{1A}, K_{1B}, K_1(1270)$ and $K_1(1400)$. Using the strong coupling constants of $D_s DK_1$, $D_s^* DK_1$ and $D_s^* D^* K_1$ vertices for $K_1(1270)$ and $K_1(1400)$ mesons, we evaluated the branching ratios of the non-leptonic decays $B^0 \rightarrow K_1^+(1270, 1400)\pi^-$. Our results for the branching ratios of these decays are in a good agreement with the experimental values.

I. INTRODUCTION

The strong coupling constants are very useful resources for understanding the nature of the strong interactions and hadronic phenomena. The strong couplings of the charmed mesons have a significant role in the hadronic decays of B meson when phenomenological models, for instance one-particle exchange model, are used. The phenomenological Lagrangian of the one-particle exchange model for the hadronic decays of B meson contains input parameters such as β and λ , which describe the strong couplings connected to the charmed mesons in these decays [1]. Therefore, the calculation of the strong form factors and coupling constants, especially vertices composed of the charmed mesons, has attracted much attention. Until now, researchers have computed some coupling constants of the charmed mesons such as $D^*D^*\rho$ [2], $D^*D\pi$ [3, 4], $DD\rho$ [5], $D^*D\rho$ [6], DDJ/ψ [7], D^*DJ/ψ [8], D^*D_sK , D_s^*DK , $D_0^*D_sK$, D_{s0}^*DK [9], D^*D^*P , D^*DV , DDV [10], $D^*D^*\pi$ [11], D_sD^*K , D_s^*DK [12], $DD\omega$ [13], D_sD_sV , $D_s^*D_s^*V$ [14, 15], and $D_1D^*\pi$, $D_1D_0\pi$, $D_1D_1\pi$ [16]. These coupling constants are often evaluated within the framework of the QCD sum rules.

In this work, we decide to calculate the strong coupling constants associated with DDa_1 , DDb_1 , D_sDK_{1A} , D_sDK_{1B} , D^*Da_1 , D^*Db_1 , $D_s^*DK_{1A}$, $D_s^*DK_{1B}$, $D^*D^*a_1$, $D^*D^*b_1$, $D_s^*D^*K_{1A}$ and $D_s^*D^*K_{1B}$ vertices in the framework of the light-cone sum rules (LCSR). Also, the strong coupling constants related to D_sDK_1 , $D_s^*DK_1$ and $D_s^*D^*K_1$ vertices for $K_1(1270)$ and $K_1(1400)$ axial vector mesons are estimated by the corresponding vertices of K_{1A} and K_{1B} mesons. For example, the relations for the coupling constants $g_{D_sDK_1(1270)}$ and $g_{D_sDK_1(1400)}$ are as

$$\begin{aligned} g_{D_sDK_1(1270)} &= g_{D_sDK_{1A}} \sin \theta_K + g_{D_sDK_{1B}} \cos \theta_K, \\ g_{D_sDK_1(1400)} &= g_{D_sDK_{1A}} \cos \theta_K - g_{D_sDK_{1B}} \sin \theta_K, \end{aligned} \quad (1)$$

where θ_K is the mixing angle. Similar expressions can be written for $f_{D_s^*DK_1(1270,1400)}$ and $h_{D_s^*D^*K_1(1270,1400)}$.

As an example of specific application of these coupling constants can be pointed out to branching ratio calculations of hadronic B decays. In this paper, we would like to consider the branching ratios of the decays

$$B^0 \rightarrow K_1^+(1270, 1400)\pi^-,$$

according to the coupling constants of D_sDK_1 , $D_s^*DK_1$ and $D_s^*D^*K_1$ vertices.

The plan of the present paper is as follows: In section II, the strong coupling constants g_{DDA} , f_{D^*DA} and $h_{D^*D^*A}$ are calculated in the framework of the LCSR. In section III, we analyze and estimate the strong coupling constants for the aforementioned vertices. In addition, we consider the branching ratio of $B^0 \rightarrow K_1^+\pi^-$ decay for $K_1(1270)$ and $K_1(1400)$ mesons using the coupling constants of D_sDK_1 , $D_s^*DK_1$ and $D_s^*D^*K_1$ vertices and compare our results with the experimental values and predictions of other methods.

II. STRONG COUPLING CONSTANTS IN THE LCSR

In the LCSR, the strong coupling constants $g_{D(s)DA}$, $f_{D(s)^*DA}$ and $h_{D(s)^*D^*A}$ are evaluated with $\Pi^{D(s)DA}$, $\Pi_\mu^{D(s)^*DA}$ and $\Pi_{\mu\nu}^{D(s)^*D^*A}$ correlation functions, respectively. From now on for simplicity, we use $D(D^*)$ instead of $D^0(D^{*0})$, $D^+(D^{*+})$

^{*} e-mail: samira.momeni@ph.iut.ac.ir

[†] e-mail: rezakhosravi@iut.ac.ir

and $D_s(D_s^*)$ in our formulations. The aforementioned correlation functions are defined as

$$\begin{aligned}\Pi^{DDA}(p, q) &= i \int d^4x e^{-iq \cdot x} \langle 0 | \mathcal{T} \{ j^D(0) j^{D^\dagger}(x) \} | A(p) \rangle, \\ \Pi_\mu^{D^*DA}(p, q) &= i \int d^4x e^{-iq \cdot x} \langle 0 | \mathcal{T} \{ j_\mu^{D^*}(0) j^{D^\dagger}(x) \} | A(p) \rangle, \\ \Pi_{\mu\nu}^{D^*D^*A}(p, q) &= i \int d^4x e^{-iq \cdot x} \langle 0 | \mathcal{T} \{ j_\mu^{D^*}(0) j_\nu^{D^* \dagger}(x) \} | A(p) \rangle,\end{aligned}\quad (2)$$

where \mathcal{T} is the time-ordering operator. In addition, $j^D = i\bar{q}_i(1-\gamma_5)c$ and $j_\mu^{D^*} = i\bar{q}_i\gamma_\mu c$ (q_i is the field of the light quark from which the charmed meson is made; u, d , or s) are the interpolating currents for D and D^* mesons, respectively. The main reason for choosing the Chiral current $i\bar{q}_i(1-\gamma_5)c$ for D meson instead of the usual pseudoscalar current $i\bar{q}_i\gamma_5c$ is to provide the results with less uncertainties [17].

In the LCSR approach, the correlation functions Π^{DDA} , $\Pi_\mu^{D^*DA}$ and $\Pi_{\mu\nu}^{D^*D^*A}$ can be calculated in two different ways. In the physical or phenomenological representation and the QCD or theoretical ones. The strong coupling constants g_{DDA} , f_{D^*DA} and $h_{D^*D^*A}$ can be obtained by using the dispersion relation to link these two representations of the correlation functions.

A. The phenomenological side

In the phenomenological part, DDA , D^*DA and D^*D^*A vertices can be studied in terms of hadronic parameters. To obtain the phenomenological side of the correlation functions, we can insert two complete sets of intermediate states with the same quantum numbers as the meson currents into these correlation functions. After isolating the higher-state contributions from the pole terms of charmed mesons and performing the Fourier transformation, we have:

$$\begin{aligned}\Pi^{DDA}(p, q) &= \frac{\langle 0 | j^D | D(p+q) \rangle \langle D(p+q) | A(p) D(q) \rangle \langle D(q) | j^{D^\dagger} | 0 \rangle}{(m_D^2 - q^2) [m_D^2 - (p+q)^2]} + \text{higher and continuum states}, \\ \Pi_\mu^{D^*DA}(p, q) &= \frac{\langle 0 | j_\mu^{D^*} | D^*(p+q) \rangle \langle D^*(p+q) | A(p) D(q) \rangle \langle D(q) | j^{D^\dagger} | 0 \rangle}{(m_{D^*}^2 - q^2) [m_{D^*}^2 - (p+q)^2]} + \text{higher and continuum states}, \\ \Pi_{\mu\nu}^{D^*D^*A}(p, q) &= \frac{\langle 0 | j_\mu^{D^*} | D^*(p+q) \rangle \langle D^*(p+q) | A(p) D^*(q) \rangle \langle D^*(q) | j_\nu^{D^* \dagger} | 0 \rangle}{(m_{D^*}^2 - q^2) [m_{D^*}^2 - (p+q)^2]} + \text{higher and continuum states}.\end{aligned}\quad (3)$$

Using the following matrix elements:

$$\begin{aligned}\langle 0 | j^D(0) | D(p+q) \rangle &= \frac{f_D m_D^2}{m_c + m_{q_i}}, \\ \langle D(p+q) | A(p) D(q) \rangle &= 2 g_{DDA} \varepsilon \cdot q, \\ \langle 0 | j_\mu^{D^*}(0) | D^*(p+q) \rangle &= f_{D^*} m_{D^*} \varepsilon_\mu^*, \\ \langle D^*(p+q) | A(p) D(q) \rangle &= 4i f_{D^*DA} \epsilon^{\alpha\beta\sigma\lambda} p_\alpha q_\beta \varepsilon_\sigma^* \varepsilon_\lambda, \\ \langle D^*(p+q) | A(p) D^*(q) \rangle &= i h_{D^*D^*A} [(p+2q)^\alpha g^{\beta\lambda} + (p+q)^\beta g^{\lambda\alpha} + q^\lambda g^{\alpha\beta}] \varepsilon_\alpha^* \varepsilon_\beta \varepsilon_\lambda^*(q),\end{aligned}\quad (4)$$

where ε^* , ε and $\varepsilon^*(q)$ represent the polarizations of $D^*(p+q)$, A and $D^*(q)$ mesons respectively, the following results are obtained:

$$\begin{aligned}\Pi^{DDA}(p, q) &= \frac{2 f_D^2 m_D^4}{(m_c + m_{q_i})^2 (m_D^2 - q^2) [m_D^2 - (p+q)^2]} g_{DDA} \varepsilon \cdot q + \text{higher and continuum states}, \\ \Pi_\mu^{D^*DA}(p, q) &= \frac{4i f_D f_{D^*} m_D^2 m_{D^*}}{(m_c + m_{q_i}) (m_D^2 - q^2) [m_{D^*}^2 - (p+q)^2]} f_{D^*DA} \epsilon_{\mu\lambda\alpha\beta} \varepsilon^\lambda p^\alpha q^\beta + \text{higher and continuum states}, \\ \Pi_{\mu\nu}^{D^*D^*A}(p, q) &= \frac{i f_{D^*}^2 m_{D^*}^2}{(m_{D^*}^2 - q^2) [m_{D^*}^2 - (p+q)^2]} h_{D^*D^*A} (p+q)_\mu \varepsilon_\nu + \text{higher and continuum states},\end{aligned}\quad (5)$$

where g_{DDA} , f_{D^*DA} and $h_{D^*D^*A}$ are the strong coupling constants, m_D , m_{D^*} and f_D , f_{D^*} are masses and decay constants of mesons, respectively. Any arbitrary structure in the correlation function can be selected to compute the strong coupling. Here, calculations are done for the Lorentz structures $\varepsilon \cdot q$, $\epsilon_{\mu\lambda\alpha\beta} \varepsilon^\lambda p^\alpha q^\beta$ and $(p+q)_\mu \varepsilon_\nu$ from Π^{DDA} , $\Pi_\mu^{D^*DA}$ and $\Pi_{\mu\nu}^{D^*D^*A}$, respectively.

B. The theoretical side

To calculate the QCD or the theoretical part of Π^{DDA} , $\Pi_\mu^{D^*DA}$ and $\Pi_{\mu\nu}^{D^*D^*A}$ in the LCSR approach, the \mathcal{T} product of the interpolating currents should be expanded at the light-like distances $x^2 \simeq 0$. After contracting the c quark field, the correlation functions

$$\begin{aligned}\Pi^{DDA}(p, q) &= - \int d^4x e^{-iq \cdot x} \langle 0 | \bar{q}_i(0) (1 - \gamma_5) S_c(x, 0) (1 - \gamma_5) q_j(x) | A(p) \rangle, \\ \Pi_\mu^{D^*DA}(p, q) &= - \int d^4x e^{-iq \cdot x} \langle 0 | \bar{q}_i(0) \gamma_\mu S_c(x, 0) (1 - \gamma_5) q_j(x) | A(p) \rangle, \\ \Pi_{\mu\nu}^{D^*D^*A}(p, q) &= - \int d^4x e^{-iq \cdot x} \langle 0 | \bar{q}_i(0) \gamma_\mu S_c(x, 0) \gamma_\nu q_j(x) | A(p) \rangle,\end{aligned}\quad (6)$$

are obtained. In these phrases, $S_c(x, 0)$ is the propagator of c quark, q_i and q_j are the fields of the light quarks that are located inside the two charmed mesons. For calculating the theoretical part of the correlation function, the Fierz rearrangement is utilized. As a result of the Fierz rearrangement, the combination of $\Gamma^\lambda \Gamma_\lambda$ is appeared before $q_j(x)$ in the correlation functions, where Γ_λ is the full set of the Dirac matrices, $\Gamma_\lambda = (I, \gamma_5, \gamma_\mu, \gamma_\mu \gamma_5, \sigma_{\mu\nu})$. After rearrangement the quantum fields and matrices, the correlation functions turn into two parts including a trace section and a matrix element of nonlocal operators between A meson and vacuum state, as

$$\begin{aligned}\Pi^{DDA}(p, q) &= \frac{i}{4} \int d^4x \int \frac{d^4k}{(2\pi)^4} \frac{e^{i(k-q) \cdot x}}{k^2 - m_c^2} \text{Tr} (1 - \gamma_5) (\not{k} + m_c) (1 - \gamma_5) \Gamma^\lambda \langle 0 | \bar{q}_i(0) \Gamma_\lambda q_j(x) | A(p) \rangle, \\ \Pi_\mu^{D^*DA}(p, q) &= \frac{i}{4} \int d^4x \int \frac{d^4k}{(2\pi)^4} \frac{e^{i(k-q) \cdot x}}{k^2 - m_c^2} \text{Tr} \gamma_\mu (\not{k} + m_c) (1 - \gamma_5) \Gamma^\lambda \langle 0 | \bar{q}_i(0) \Gamma_\lambda q_j(x) | A(p) \rangle, \\ \Pi_{\mu\nu}^{D^*D^*A}(p, q) &= \frac{i}{4} \int d^4x \int \frac{d^4k}{(2\pi)^4} \frac{e^{i(k-q) \cdot x}}{k^2 - m_c^2} \text{Tr} \gamma_\mu (\not{k} + m_c) \gamma_\nu \Gamma^\lambda \langle 0 | \bar{q}_i(0) \Gamma_\lambda q_j(x) | A(p) \rangle.\end{aligned}\quad (7)$$

In the LCSR approach the non-zero matrix elements $\langle 0 | \bar{q}_i(0) \Gamma_\lambda q_j(x) | A(p) \rangle$, called the light-cone distribution amplitudes (LCDAs), are defined in terms of twist functions. For instance, the two-parton distribution amplitude for the axial vector meson A , with the light quark content q_i and q_j , is given as [18]:

$$\begin{aligned}\langle 0 | \bar{q}_i^\alpha(0) q_j^\delta(x) | A(p, \varepsilon) \rangle &= -\frac{i}{4} \int_0^1 du e^{-iup \cdot x} \left\{ f_A m_A \left[\not{p} \gamma_5 \frac{\varepsilon \cdot x}{p \cdot x} \Phi_{\parallel}(u) + \left(\not{\varepsilon} - \not{p} \frac{\varepsilon \cdot x}{p \cdot x} \right) \gamma_5 g_{\perp}^{(a)}(u) \right. \right. \\ &\quad \left. \left. - \not{x} \gamma_5 \frac{\varepsilon \cdot x}{2(p \cdot x)^2} m_A^2 \phi_b(u) + \varepsilon_{\mu\nu\rho\sigma} \varepsilon^\nu p^\rho x^\sigma \gamma^\mu \frac{g_{\perp}^{(v)}(u)}{4} \right] \right. \\ &\quad \left. + f_A^\perp \left[\frac{1}{2} (\not{p} \not{\varepsilon} - \not{\varepsilon} \not{p}) \gamma_5 \Phi_{\perp}(u) - \frac{1}{2} (\not{p} \not{x} - \not{x} \not{p}) \gamma_5 \frac{\varepsilon \cdot x}{(p \cdot x)^2} m_A^2 \bar{h}_{\parallel}^{(t)}(u) \right. \right. \\ &\quad \left. \left. + i(\varepsilon \cdot x) m_A^2 \gamma_5 \frac{h_{\parallel}^{(p)}(u)}{2} \right] \right\}^{\delta\alpha},\end{aligned}\quad (8)$$

where Φ_{\parallel} , Φ_{\perp} are twist-2, $g_{\perp}^{(a)}$, $g_{\perp}^{(v)}$, $h_{\parallel}^{(t)}$ and $h_{\parallel}^{(p)}$ are twist-3 functions. In addition, ϕ_b and $\bar{h}_{\parallel}^{(t)}$ are defined as

$$\begin{aligned}\phi_b(u) &= \Phi_{\parallel}(u) - 2g_{\perp}^{(a)}(u), \\ \bar{h}_{\parallel}^{(t)}(u) &= h_{\parallel}^{(t)}(u) - \frac{1}{2}\Phi_{\perp}(u),\end{aligned}$$

for $x^2 \neq 0$. Moreover, f_A and f_A^\perp are the decay constants of the axial vector meson A . The explicit expressions for the relevant two-parton distribution amplitudes and definitions for the above mentioned twist functions are collected in Appendix.

After substituting the two-parton distribution amplitudes of the axial vector meson A into the correlation functions $\Pi^{DDA}(p, q)$, $\Pi_\mu^{D^*DA}$ and $\Pi_{\mu\nu}^{D^*D^*A}$, we should calculate some traces and then integrals over variables x and u . In the next step, we equate the coefficients of the structures $\varepsilon \cdot q$, $\varepsilon_{\mu\lambda\alpha\beta} \varepsilon^\lambda p^\alpha q^\beta$ and $(p+q)_\mu \varepsilon_\nu$ from both the phenomenological and theoretical sides of $\Pi^{DDA}(p, q)$, $\Pi_\mu^{D^*DA}$ and $\Pi_{\mu\nu}^{D^*D^*A}$, respectively. Finally, to apply the Borel transformations

with respect to two variables $(p+q)^2$ and q^2 , the strong couplings g_{DDA} , f_{D^*DA} and $h_{D^*D^*A}$ are obtained in the LCSR as

$$\begin{aligned} g_{DDA} &= \frac{\Delta(u_0, s_0) f_A^\perp}{8\delta_1} \exp\left[\frac{m_D^2}{M_1^2} + \frac{m_D^2}{M_2^2}\right] \left[m_A^2 m_c (2 - u_0) h_{\parallel}^{(p)}(u_0)\right], \\ f_{D^*DA} &= \frac{\Delta(u_0, s_0) M_0^2 f_A}{8\delta_2} \exp\left[\frac{m_{D^*}^2}{M_1^2} + \frac{m_{D^*}^2}{M_2^2}\right] \left[5 \frac{f_A^\perp}{f_A} \Phi_{\perp}(u_0) + \frac{m_A m_c}{M_0^2} g_{\perp}^{(v)}(u_0)\right], \\ h_{D^*D^*A} &= \frac{\Delta(u_0, s_0) M_0^2 f_A^\perp m_c}{\delta_3} \exp\left[\frac{m_{D^*}^2}{M_1^2} + \frac{m_{D^*}^2}{M_2^2}\right] \left[2\Phi_{\perp}(u_0) + \frac{m_A^2}{M_0^2} \bar{h}_{\parallel}^{(t)(ii)}(u_0)\right], \end{aligned} \quad (9)$$

where

$$\begin{aligned} \delta_1 &= \frac{f_D^2 m_D^4}{(m_c + m_{q_i})(m_c + m_{q_j})}, & \delta_2 &= \frac{f_{D^*} f_D m_{D^*} m_D^2}{(m_c + m_{q_i})}, \\ \delta_3 &= f_{D^*}^2 m_{D^*}^2, & u_0 &= \frac{M_1^2}{M_1^2 + M_2^2}, \\ M_0^2 &= \frac{M_1^2 M_2^2}{M_1^2 + M_2^2}, & \bar{h}_{\parallel}^{(t)(ii)}(u) &= \int_0^u dv \int_0^v d\omega \bar{h}_{\parallel}^{(t)}(\omega), \\ \Delta(u_0, s_0) &= \exp\left[-\frac{u_0(1-u_0)m_A^2 + m_c^2}{M_0^2}\right] - \exp\left[-\frac{s_0}{M_0^2}\right]. \end{aligned}$$

Parameter s_0 is the continuum threshold that appears in function $\Delta(u_0, s_0)$. To calculate the coupling constant of vertex $DDA(D_s DA)$ in Eq. (9), the continuum threshold s_0 is connected to $D(D_s)$. On the other hand, in vertices $D^*DA(D_s^* DA)$ and $D^*D^*A(D_s^* D^* A)$, it is related to $D^*(D_s^*)$ meson. The continuum thresholds for the charmed mesons have been calculated via the QCD sum rules (SR) in Ref. [19]. Their results for $\sqrt{s_0}$ are presented in Table I.

TABLE I: The continuum threshold parameters for D , D_s , D^* and D_s^* mesons in GeV.

Meson	D	D_s	D^*	D_s^*
$\sqrt{s_0}$	2.45 ± 0.15	2.50 ± 0.20	2.55 ± 0.05	2.56 ± 0.15

The Borel transformations, used in extracting the strong coupling relations in Eq. (9), are as follows.

$$B_{\Lambda^2}(M^2) \left[\frac{1}{\Lambda^2 - m^2} \right] = -\frac{e^{-\frac{m^2}{M^2}}}{M^2}, \quad B_{\Lambda^2}(M^2) \left[e^{-\alpha \Lambda^2} \right] = \delta(1 - \alpha M^2),$$

where Λ is variable. In the Borel transformations, parameter M is known as the Borel mass.

Now, the values of the strong couplings g_{DDa_1} , g_{DDb_1} , $g_{D_s DK_{1A}}$, $g_{D_s DK_{1B}}$, $f_{D^*Da_1}$, $f_{D^*Db_1}$, $f_{D_s^* DK_{1A}}$, $f_{D_s^* DK_{1B}}$, $h_{D^*D^*a_1}$, $h_{D^*D^*b_1}$, $h_{D_s^* D^* K_{1A}}$ and $h_{D_s^* D^* K_{1B}}$ can be estimated numerically, with the help of Eq. (9) obtained using the LCSR. In addition, the results of the strong couplings $g_{D_s DK_1}$, $f_{D_s^* DK_1}$ and $h_{D_s^* D^* K_1}$ for $K_1(1270)$ and $K_1(1400)$ mesons are calculated by Eq. (1).

III. NUMERICAL ANALYSIS

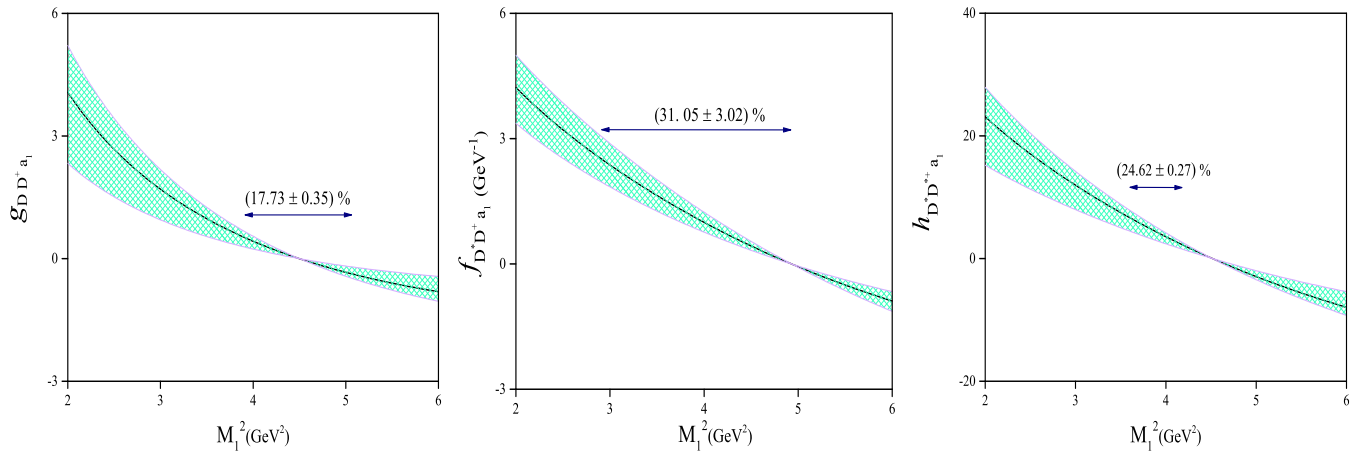
In this section, our numerical analysis is presented for the strong coupling constants g_{DDA} , f_{D^*DA} and $h_{D^*D^*A}$. In this work, the masses of the light quarks u and d are neglected. The masses for s and c quarks are taken in GeV as $m_s = (0.09 \pm 0.00)$ and $m_c = (1.28 \pm 0.03)$, respectively [20]. For charmed mesons, the masses are used in GeV as $m_D = 1.86$, $m_{D_s} = 1.96$, $m_{D^*} = 2.01$ and $m_{D_s^*} = 2.11$ [20]. In this work, the decay constant values of the charmed mesons $D^{(*)}$ and $D_s^{(*)}$, obtained in the SR, are used as $f_D = (201 \pm 13)$ MeV, $f_{D_s} = (238 \pm 23)$ MeV, $f_{D^*} = (242 \pm 20)$ MeV and $f_{D_s^*} = (314 \pm 19)$ MeV [21]. The decay constant values of the axial vector mesons, i.e. f_A and f_A^\perp are equal at energy scale $\mu = 1$ GeV. The masses and the decay constant values for the axial vector mesons, evaluated from the LCSR [18], are presented in Table II.

A. Analysis of the strong coupling constants g_{DDA} , f_{D^*DA} and $h_{D^*D^*A}$

Having all the input parameters, we are ready to do numerical analysis for the coupling constants. The coupling constants g_{DDA} , f_{D^*DA} and $h_{D^*D^*A}$ in Eq. (9) contain two Borel parameters M_1^2 and M_2^2 . These are not physical

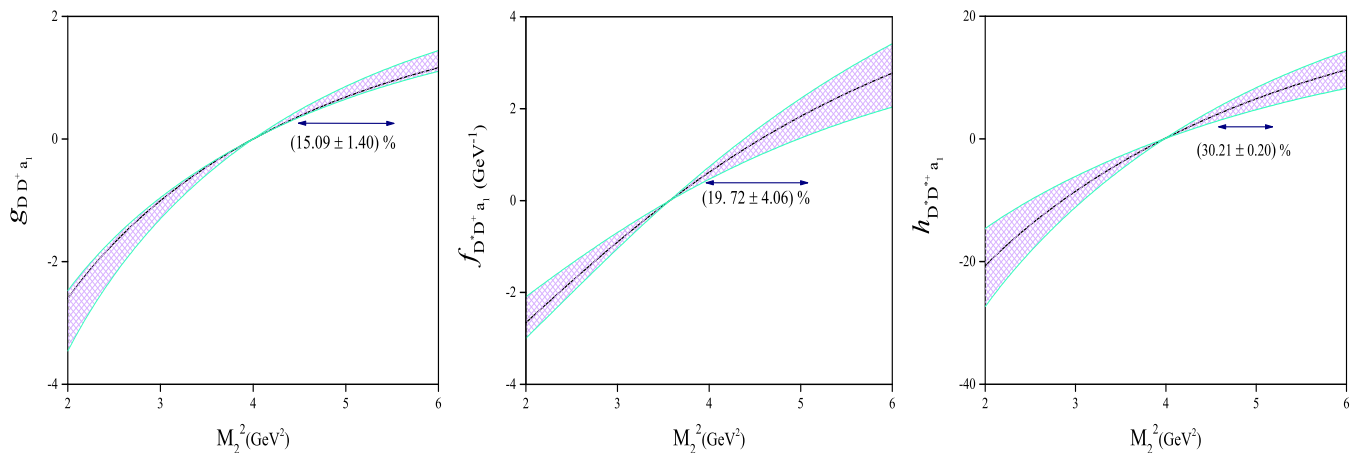
TABLE II: Masses and decay constant values for axial vector mesons a_1, b_1, K_{1A}, K_{1B} .

Axial vector meson	a_1	b_1	K_{1A}	K_{1B}
m_A (GeV)	1.23 ± 0.40	1.23 ± 0.32	1.31 ± 0.06	1.34 ± 0.08
f_A (MeV)	238 ± 10	180 ± 8	250 ± 13	190 ± 10

FIG. 1: Strong coupling constants $g_{DD^*a_1}$, $f_{D^*D^*a_1}$ and $h_{D^*D^*a_1}$ with their errors as a function of Borel mass M_1^2 . For all the strong coupling constants, Borel parameter M_2^2 is fixed at 4.5 GeV^2 .

quantities, so the coupling constants should be independent of them. For instance, the dependence of the strong couplings $g_{DD^*a_1}$, $f_{D^*D^*a_1}$ and $h_{D^*D^*a_1}$ on Borel mass parameters M_1^2 and M_2^2 are shown in Figs. 1 and 2, respectively. In these figures, the black lines show the central values of the coupling constants. The shaded regions are obtained by using the errors of the input parameters. As can be seen in Figs. 1 and 2, the strong couplings $g_{DD^*a_1}$, $f_{D^*D^*a_1}$ and $h_{D^*D^*a_1}$ can be stable within the Borel mass intervals $4 [4.5] \text{ GeV}^2 < M_1^2 [M_2^2] < 5 [5.5] \text{ GeV}^2$, $3 [4] \text{ GeV}^2 < M_1^2 [M_2^2] < 5 [5] \text{ GeV}^2$, and $3.5 [4.5] \text{ GeV}^2 < M_1^2 [M_2^2] < 4.5 [5.5] \text{ GeV}^2$, respectively. The percentage of the coupling constant variations at the suitable intervals of the Borel parameters is displayed in each plot. The main uncertainty in $g_{DD^*a_1}$ comes from c quark mass (m_c) and the Gegenbauer moments a_0^\perp , a_1^\perp and a_2^\perp of $h_\perp^{(p)}$ LCDA, while for $f_{D^*D^*a_1}$ and $h_{D^*D^*a_1}$, the main sources of uncertainties are the c quark mass and Φ_\perp LCDA.

Taking all values and parameters and their uncertainties in Eq. (9), the values for the strong coupling constants are obtained and shown in Table III. It is worth mentioning that the strong coupling constants $g_{DD^*a_1}$ and $h_{D^*D^*a_1}$

FIG. 2: The same as Fig. 1 but for Borel mass M_2^2 . For all the strong coupling constants the suitable regions for Borel parameter M_1^2 are shown in Fig 1.

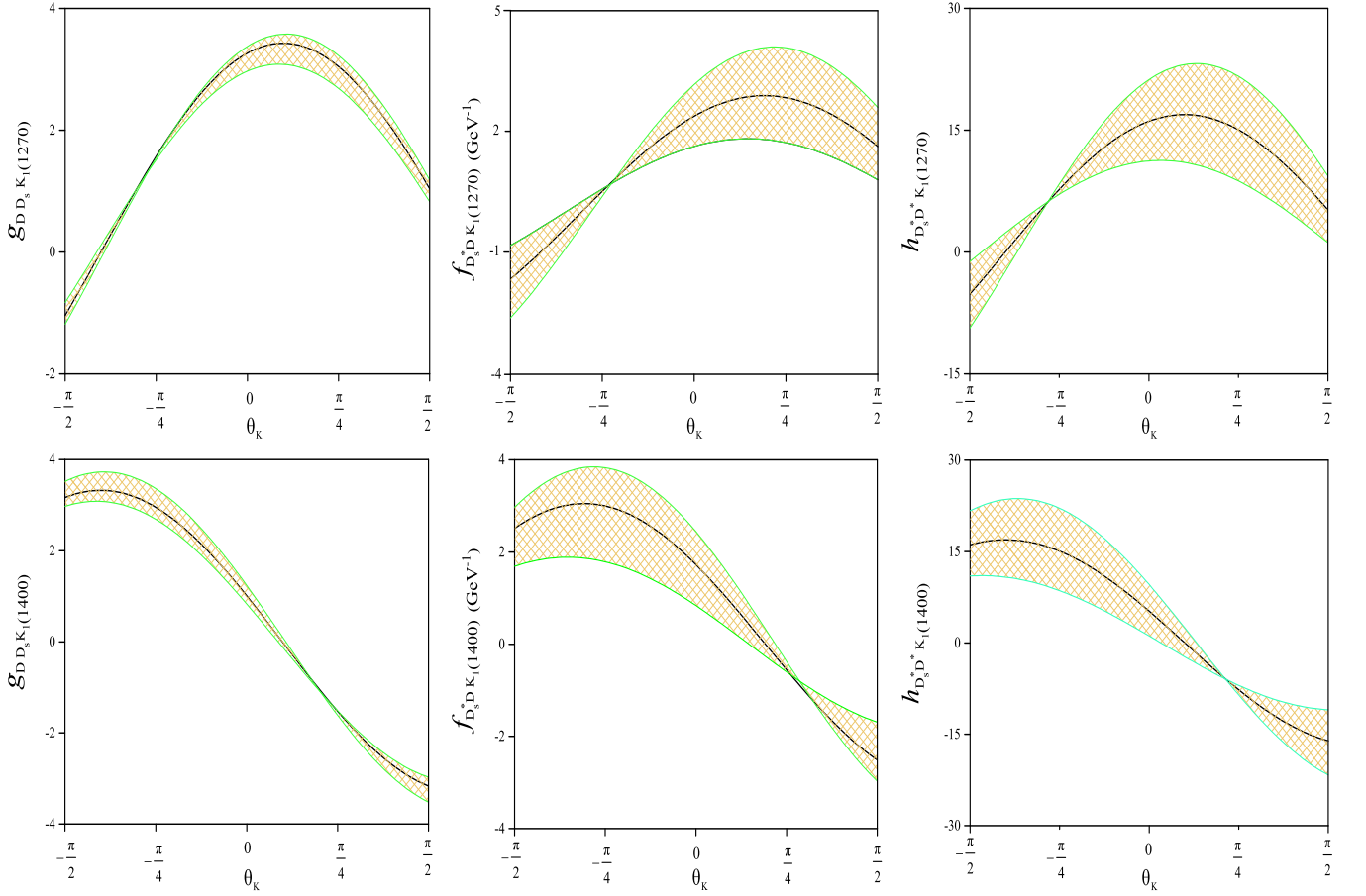


FIG. 3: The strong coupling constants $g_{D_s D^* K_1}$, $f_{D_s^* D K_1}$ and $h_{D_s^* D^* K_1}$ for $K_1(1270)$ and $K_1(1400)$ as a function of the mixing angle θ_K .

are dimensionless.

TABLE III: The values of the strong coupling constants g_{DDA} , $f_{D^*DA}(\text{GeV}^{-1})$ and $h_{D^*D^*A}$ obtained in the LCSR calculation with their uncertainties.

A	a_1	b_1	K_{1A}	K_{1B}
g_{DDA}	0.38 ± 0.07	1.64 ± 0.15	1.17 ± 0.49	1.51 ± 0.11
f_{D^*DA}	1.03 ± 0.25	1.90 ± 0.72	1.36 ± 0.78	2.48 ± 0.78
$h_{D^*D^*A}$	3.67 ± 1.01	6.32 ± 1.75	2.86 ± 0.95	6.59 ± 2.02

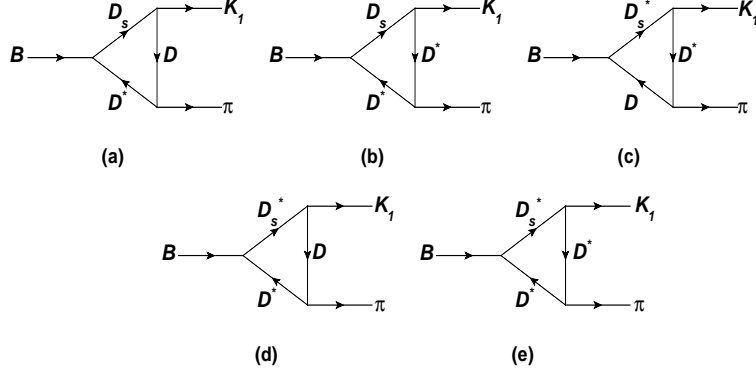
Mesons a_1 and ρ have the same quark content, but different masses and parities, i.e. ρ is a vector (1^-) and a_1 is an axial vector (1^+). The values of the strong couplings $g_{DD\rho}$, $f_{D^*D\rho}$ and $h_{D^*D^*\rho}$ are evaluated as (1.31 ± 0.29) , $(0.89 \pm 0.15) \text{ GeV}^{-1}$ and (6.6 ± 0.31) using the SR method in Refs. [22, 23]. According to Table III, only the strong couplings $f_{D^*Da_1}$ and $f_{D^*D\rho}$ are approximately equal.

The strong coupling constants $g_{D_s D^* K_1}$, $f_{D_s^* D K_1}$ and $h_{D_s^* D^* K_1}$ for $K_1(1270)$ and $K_1(1400)$ are plotted in Fig. 3, as a function of the mixing angle θ_K . The uncertainty regions are also displayed in this figure.

The values of the strong couplings $g_{D_s D^* K_1}$, $f_{D_s^* D K_1}$ and $h_{D_s^* D^* K_1}$ depend on the mixing angle θ_K . The mixing angle θ_K can be determined by the experimental data [24–27]. A new research for the value of θ_K indicates that this mixing angle is around either $\pm 33^\circ$ or $\pm 58^\circ$ [28, 29]. On the other hand, the recent experimental values for the branching ratios of the $B \rightarrow K_1(1270, 1400)\pi$ decays are reported at $\theta_K = (72 \pm 3)^\circ$ by BABAR [30]. For the next calculations and comparisons, we need the values of the aforementioned coupling constants at $\theta_K = -58^\circ, -37^\circ, -33^\circ, 32^\circ$ and 72° . Therefore, these values are presented in Table IV.

TABLE IV: Values of the strong coupling constants $g_{D_s D K_1}$, $f_{D_s^* D K_1}$ (GeV^{-1}), and $h_{D_s^* D^* K_1}$ at the various mixing angles.

θ_K	-58°	-37°	-33°	32°	72°
$g_{D_s D K_1(1270)}$	0.87 ± 0.05	1.94 ± 0.20	1.95 ± 0.25	3.31 ± 0.26	1.98 ± 0.19
$f_{D_s^* D K_1(1270)}$	-0.10 ± 0.35	0.88 ± 0.08	2.39 ± 1.12	2.98 ± 1.16	2.29 ± 1.01
$h_{D_s^* D^* K_1(1270)}$	2.23 ± 0.79	9.52 ± 1.38	10.20 ± 5.58	16.37 ± 6.28	9.91 ± 5.35
$g_{D_s D K_1(1400)}$	3.21 ± 0.26	2.73 ± 0.38	-2.59 ± 0.16	-0.84 ± 0.05	-2.69 ± 0.13
$f_{D_s^* D K_1(1400)}$	2.89 ± 0.81	2.75 ± 0.88	-1.71 ± 0.35	0.10 ± 0.30	-1.76 ± 0.40
$h_{D_s^* D^* K_1(1400)}$	16.37 ± 7.05	7.63 ± 5.02	-13.68 ± 3.49	-4.23 ± 0.69	-13.69 ± 3.02

FIG. 4: Diagrams for the $B \rightarrow K_1 \pi$ decay with $D_s^{(*)}$ and $D^{(*)}$ intermediate states.

B. Branching ratio analysis of the non-leptonic $B^0 \rightarrow K_1^+ \pi^-$ decay

In this section, we want to evaluate the branching ratio values for the non-leptonic $B^0 \rightarrow K_1^+(1270, 1400)\pi^-$ decays. According to Refs. [31, 32], the amplitude of $B^0 \rightarrow K_1^+ \pi^-$ decay, $\mathcal{M}_{K_1 \pi}$, is written in two parts; the short-distance contribution (SD) and the long-distance ones (LD), as:

$$\mathcal{M}_{K_1 \pi} = \mathcal{M}_{SD} + \mathcal{M}_{LD}. \quad (10)$$

In the above phrase, \mathcal{M}_{SD} is written using the effective Hamiltonian for the non-leptonic B decays in the factorization approximation as [33–37]:

$$\mathcal{M}_{SD}(B^0 \rightarrow K_1^+ \pi^-) = G_F \sqrt{2} F_1^{B \rightarrow \pi}(m_{K_1}^2) f_{K_1} m_{K_1} \left[V_{ub}^* V_{us} a_2 - V_{tb}^* V_{ts} (a_4 + a_{10}) \right] (\varepsilon \cdot p_B), \quad (11)$$

where G_F is the Fermi constant, V_{ij} is the CKM matrix element, ε is the polarization vector of K_1 meson and $a_i = C_i + \frac{C_{i-1}}{3}$ (C_i is the Wilson coefficient). In addition $F_1^{B \rightarrow \pi}(m_{K_1}^2)$ is the transition form factor of the semileptonic $B \rightarrow \pi$ decay estimated in $m_{K_1}^2$ [38].

For the long-distance part of the amplitude, diagrams displayed in Fig. 4 are considered. As shown in this figure, $D_s^{(*)}$ and $D^{(*)}$ mesons are considered as the intermediate states in the decay process of B^0 to $K_1^+ \pi^-$; first, B meson decays into a $D_s^{(*)} D^{(*)}$ intermediate states, and then these two particles produce the final mesons K_1 and π by exchanging a $D^{(*)}$ meson. In this view, the \mathcal{M}_{LD} is given by the following formula:

$$\mathcal{M}_{LD} = \text{Re}(\mathcal{M}_{LD}) + \text{Im}(\mathcal{M}_{LD}). \quad (12)$$

Using the charming penguin diagrams in Fig. 4, the imaginary part of \mathcal{M}_{LD} can be computed as

$$\text{Im}(\mathcal{M}_{LD}) = \frac{m_D}{32\pi^2 m_B} \sqrt{\omega^{*2} - 1} \int d\mathbf{n} \mathcal{M} [B(v) \rightarrow D_s^{(*)}(q) D^{(*)}(v')] \mathcal{M} [D_s^{(*)} D^{(*)} \rightarrow K_1 \pi], \quad (13)$$

where the integration is over the solid angle. The amplitude for $B \rightarrow D_s^{(*)} D^{(*)}$ transition is computed as

$$\mathcal{M} [B(v) \rightarrow D_s(q) D^*(\varepsilon^*, v')] = -K (m_B + m_{D_s}) \varepsilon \cdot v, \quad (14)$$

$$\mathcal{M} [B(v) \rightarrow D_s^*(\varepsilon, q) D(v')] = -K m_{D_s^*} \varepsilon \cdot (v + v'), \quad (15)$$

$$\mathcal{M} [B(v) \rightarrow D_s^*(\varepsilon, q) D^*(\varepsilon^*, v')] = -iK m_{D_s^*} \varepsilon^\mu \varepsilon^{*\alpha} (i \varepsilon_{\alpha\lambda\mu\sigma} v'^\lambda v^\sigma - g_{\mu\alpha} (1 + \omega^*) + v_\alpha v'_\mu). \quad (16)$$

In these phrases K and ω^* are as follows:

$$K = \frac{\sqrt{2}G_F a_2}{1 + \omega^*} V_{cb}^* V_{cs} \sqrt{m_B m_{D^*}} f_{D_s^{(*)}}, \quad \omega^* = \frac{m_B^2 + m_{D^{(*)}}^2 - m_{D_s^{(*)}}^2}{2m_{D^{(*)}} m_B}. \quad (17)$$

It should be recalled that the factorization with the following kinematics are used to compute $\mathcal{M}[B \rightarrow D_s^{(*)} D^{(*)}]$:

$$p^\mu = m_B v^\mu = (m_B, \vec{0}), \quad p'^\mu = m_{D^{(*)}} v'^\mu, \quad q = p - p'. \quad (18)$$

On the other hand, the heavy quark effective lagrangian is used to estimate $\mathcal{M}[D_s^{(*)} D^{(*)} \rightarrow K_1 \pi]$. The result for the sum of diagrams (a) and (b) in Fig. 4 is obtained as

$$\begin{aligned} \mathcal{M}^{(a+b)} [D_s(q) D^*(\varepsilon^*, v') \rightarrow K_1(p_{K_1}, \varepsilon) \pi(p_\pi)] &= -\frac{\sqrt{2}g F^2(|\vec{p}_\pi|)}{f_\pi} g_V \sqrt{\frac{m_{D^*}}{m_{D_s}}} \varepsilon_\eta^* \varepsilon_\sigma \\ &\times \left\{ \frac{2\beta_1 m_{D_s} q^\sigma p_\pi^\eta}{(m_{D_s} v' - p_\pi)^2 - m_{D_s}^2} + \frac{4\lambda m_{D^*} G^{\sigma\eta}(p_\pi, p_{K_1}, v')}{(m_{D^*} v' - p_\pi)^2 - m_{D^*}^2} \right\}, \quad (19) \end{aligned}$$

where $F(|\vec{p}_\pi|) = 0.065$ [32], $g_V \simeq 5.8$ [39], $g = 0.59 \pm 0.07 \pm 0.01$ [40]. For diagram (c), amplitude is obtained as:

$$\begin{aligned} \mathcal{M}^{(c)} [D_s^*(\varepsilon^*, q) D(v') \rightarrow K_1(p_{K_1}, \varepsilon) \pi(p_\pi)] &= -\frac{\sqrt{2}g m_{D^*} F^2(|\vec{p}_\pi|)}{f_\pi} g_V \sqrt{\frac{m_{D^*}}{m_{D_s}}} \frac{\varepsilon_\eta^* \varepsilon_\sigma}{(m_{D_s^*} v' - p_\pi)^2 - m_{D_s^*}^2} \\ &\times \left\{ 2\beta_1 q^\sigma \left(p_\pi^\eta - \frac{v' \cdot p_\pi}{m_{D_s^*}} p_{K_1}^\eta \right) - 4\lambda m_{D_s^*} H^{\sigma\eta}(p_\pi, p_{K_1}, v') \right\}, \quad (20) \end{aligned}$$

and finally, the sum of diagrams (d) and (e) leads to:

$$\begin{aligned} \mathcal{M}^{(d+e)} [D_s^*(\varepsilon^*, q) D^*(\varepsilon^*, v') \rightarrow K_1(p_{K_1}, \varepsilon) \pi(p_\pi)] &= \frac{\sqrt{2}g m_{D^*} F^2(|\vec{p}_\pi|)}{f_\pi} g_V \sqrt{\frac{m_{D^*}}{m_{D_s}}} \varepsilon^{\alpha\mu\nu\eta} \varepsilon_\tau^* \varepsilon_\sigma \hat{\varepsilon}_\rho^* \\ &\times \left\{ \frac{q_\alpha (p_{K_1})_\mu \delta_\nu^\sigma \delta_\eta^\tau}{(m_{D_s^*} v' - p_\pi)^2 - m_{D_s^*}^2} \frac{4\lambda m_{D_s^*} p_\pi^\rho}{m_{D^*}} + \frac{v'_\alpha (p_\pi)_\mu \delta_\nu^\rho}{(m_{D^*} v' - p_\pi)^2 - m_{D^*}^2} (2\beta_2 q^\sigma \delta_\eta^\tau + 4\lambda m_{D_s^*} [p_{K_1}^\tau \delta_\eta^\sigma - (p_{K_1})_\eta g^{\sigma\tau}]) \right\} \quad (21) \end{aligned}$$

In these phrases $G^{\sigma\eta}$ and $H^{\sigma\eta}$ are

$$\begin{aligned} G^{\sigma\eta}(p_\pi, p_{K_1}, v') &= -(v' \cdot q)(g^{\sigma\eta}[p_{K_1} \cdot p_\pi] - p_\pi^\sigma p_{K_1}^\eta) - (q \cdot p_\pi)(v'^\sigma p_{K_1}^\eta - g^{\sigma\eta}[v' \cdot p_{K_1}]) \\ &\quad - q^\eta (p_\pi^\sigma [p_{K_1} \cdot v'] - v'^\sigma [p_{K_1} \cdot p_\pi]), \\ H^{\sigma\eta}(p_\pi, p_{K_1}, v') &= g^{\sigma\eta}(p_{K_1} \cdot p_\pi - \frac{v' \cdot p_\pi}{m_{D_s^*}} [m_{K_1}^2 - p_{K_1} \cdot q]) - p_{K_1}^\eta (p_\pi^\sigma + \frac{v' \cdot p_\pi}{m_{D_s^*}} q^\sigma). \quad (22) \end{aligned}$$

Moreover, the parameters β and λ are related to the strong coupling constants $g_{D_s D K_1}$, $f_{D_s^* D K_1}$ and $h_{D_s^* D^* K_1}$ as

$$\beta_1 = \frac{\sqrt{2}g_{D_s D K_1}}{2g_V}, \quad \lambda = \frac{\sqrt{2}f_{D_s^* D K_1}}{2g_V}, \quad \beta_2 = \frac{\sqrt{2}h_{D_s^* D^* K_1}}{2g_V}. \quad (23)$$

Similar method of the imaginary part is used to calculate the real part of the LD amplitude ($\text{Re}(\mathcal{M}_{LD})$).

In general, \mathcal{M}_{SD} is also a complex quantity like \mathcal{M}_{LD} . The input parameters in Eq. (11) are as $G_F = 1.166 \times 10^{-5} (\text{GeV}^{-2})$, $V_{ub}^* V_{us} = 2.66 \times 10^{-3}(1 + 2.90i)$, $V_{tb}^* V_{ts} = -4.21 \times 10^{-2}$ [20], $a_2 = 1.029$, $a_4 = 0.005$, $a_{10} = -0.001$ [31], $F_1^{B \rightarrow \pi}(m_{K_{1A}}^2) = 0.32$, $F_1^{B \rightarrow \pi}(m_{K_{1B}}^2) = 0.33$ [41]. First, we plot the real and imaginary parts of \mathcal{M}_{SD} for $B^0 \rightarrow K_1^+(1270, 1400)\pi^-$ decays as a function of the mixing angle θ_K in Fig. 5. Then, to illustrate the impact of the LD in the amplitudes of $B^0 \rightarrow K_1^+(1270, 1400)\pi^-$ decays, we plot the same as Fig. 5 but for $\mathcal{M}_{K_1\pi} = \mathcal{M}_{SD} + \mathcal{M}_{LD}$ in Fig. 6.

Having $\mathcal{M}_{K_1\pi}$, the branching ratio of the non-leptonic decay $B^0 \rightarrow K_1^+ \pi^-$ is given by

$$\mathcal{BR}(B^0 \rightarrow K_1^+ \pi^-) = \frac{\tau_B}{16\pi m_B^3} |\mathcal{M}_{K_1\pi}|^2 \sqrt{\lambda(m_B^2, m_{K_1}^2, m_\pi^2)}, \quad (24)$$

where τ_B is the life time of B^0 meson and $\lambda(m_B^2, m_{K_1}^2, m_\pi^2) = m_B^4 + m_{K_1}^4 + m_\pi^4 - 2m_B^2 m_{K_1}^2 - 2m_B^2 m_\pi^2 - 2m_{K_1}^2 m_\pi^2$. The θ_K dependence of the branching ratios for the non-leptonic decays $B^0 \rightarrow K_1^+(1270)\pi^-$ and $B^0 \rightarrow K_1^+(1400)\pi^-$ with their uncertainty regions is shown in Fig. 7.

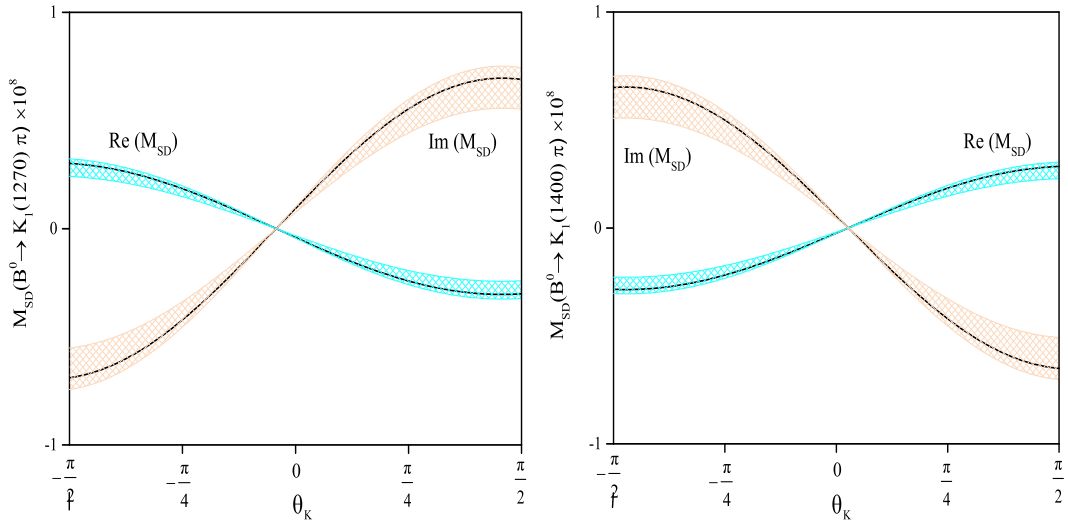


FIG. 5: The real and imaginary parts of \mathcal{M}_{SD} as a function of the mixing angle θ_K for $B^0 \rightarrow K_1^+(1270)\pi^-$ and $B^0 \rightarrow K_1^+(1400)\pi^-$ decays.

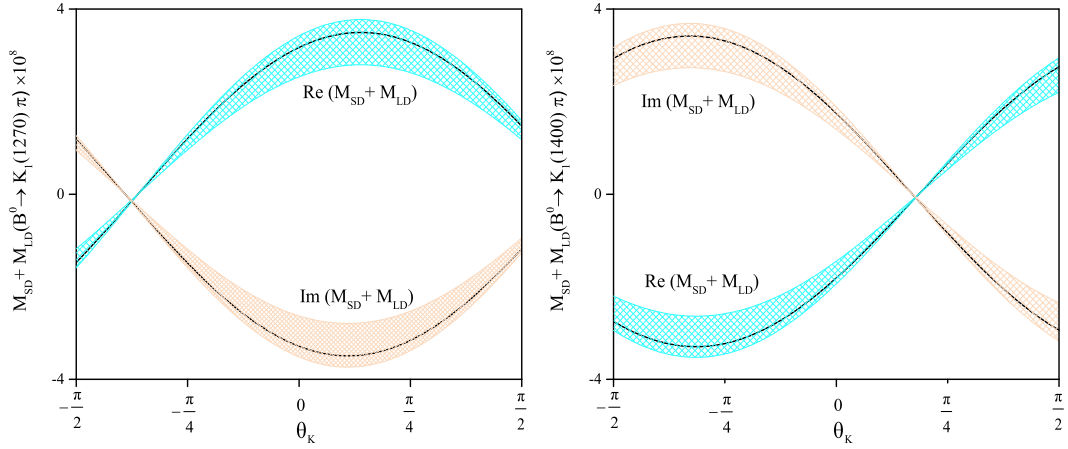


FIG. 6: The same as Fig. 5 but for $\mathcal{M}_{K_1\pi} = \mathcal{M}_{SD} + \mathcal{M}_{LD}$.

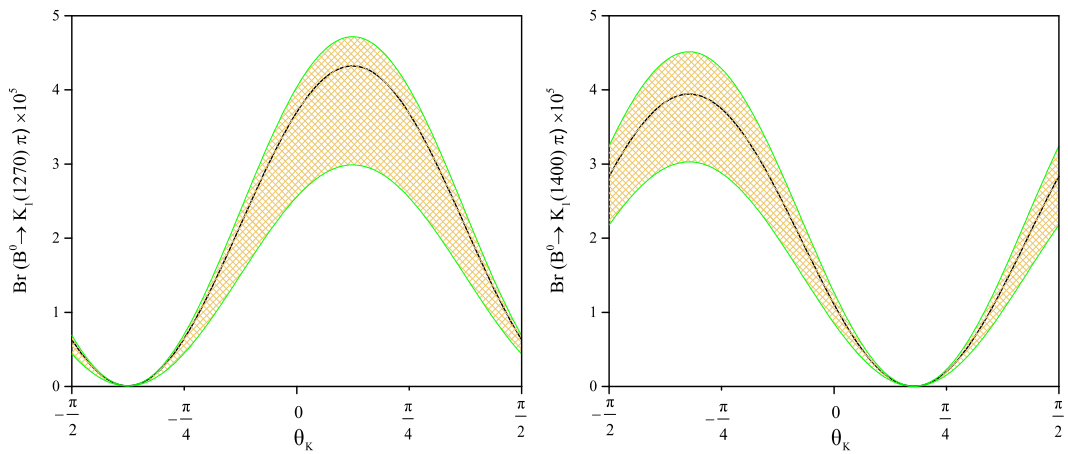


FIG. 7: Branching ratios for the non-leptonic decays $B^0 \rightarrow K_1^+(1270)\pi^-$ and $B^0 \rightarrow K_1^+(1400)\pi^-$ with respect to θ_K and their uncertainty regions.

As mentioned before, the recent experimental values for the $B^0 \rightarrow K_1^+(1270, 1400)\pi^-$ branching ratios are reported at $\theta_K = (72 \pm 3)^\circ$ by BABAR [30]. Considering the amplitudes of $B^0 \rightarrow K_1^+(1270, 1400)\pi^-$ decays in different ways such as only (\mathcal{M}_{SD}) , $(\mathcal{M}_{SD} + \mathcal{M}_{LD}^{a+b})$, $(\mathcal{M}_{SD} + \mathcal{M}_{LD}^c)$, $(\mathcal{M}_{SD} + \mathcal{M}_{LD}^{d+e})$, and the total amplitude $(\mathcal{M}_{SD} + \mathcal{M}_{LD})$, we present our results for the branching ratios at $\theta_K = (72 \pm 3)^\circ$ in Table V. According to the obtained values, $(\mathcal{M}_{SD} + \mathcal{M}_{LD}^{a+b})$ has the most contribution to our results. The experimental values for these considered decays are also reported in Table V. As can be seen, our results are in a good agreement with the experimental values.

TABLE V: Branching ratio results for $B^0 \rightarrow K_1^+(1270)\pi^-$ and $B^0 \rightarrow K_1^+(1400)\pi^-$ decays at $\theta_K = (72 \pm 3)^\circ$, in units of 10^{-5} .

Decay	Only \mathcal{M}_{SD}	$\mathcal{M}_{SD} + \mathcal{M}_{LD}^{a+b}$	$\mathcal{M}_{SD} + \mathcal{M}_{LD}^c$	$\mathcal{M}_{SD} + \mathcal{M}_{LD}^{d+e}$	$\mathcal{M}_{SD} + \mathcal{M}_{LD}$	Exp [30]
$B^0 \rightarrow K_1^+(1270)\pi^-$	0.26 ± 0.04	1.19 ± 0.11	0.53 ± 0.06	0.11 ± 0.02	1.83 ± 0.20	1.7 ± 0.4
$B^0 \rightarrow K_1^+(1400)\pi^-$	0.20 ± 0.03	1.03 ± 0.10	0.52 ± 0.05	0.08 ± 0.02	1.63 ± 0.17	1.6 ± 0.3
Sum	0.46 ± 0.07	2.22 ± 0.21	1.05 ± 0.11	0.19 ± 0.04	3.46 ± 0.37	3.2 ± 0.3

For a better analysis, other theoretical predictions for the branching ratios of $B^0 \rightarrow K_1^+(1270, 1400)\pi^-$ decays are also presented in Table VI. It is noticed that the results of Refs. [42, 43] are obtained for mixing angle 32° , while those in Ref. [44] are obtained for mixing angle -37° . Also, the mixing angle θ_K is considered in two values -33° and -58° in Ref. [45]. For a comparison, we show our results for the $B^0 \rightarrow K_1^+(1270, 1400)\pi^-$ branching ratios in the different values of the mixing angle θ_K in Table VII. As can be seen in Tables VI and VII, the values predicted by us in the different angles are in most cases greater than that those predicted by the other methods.

In summary, the strong coupling constants of DDA , D^*D^*A and D^*DA vertices were considered in the framework of the LCSR, where A is an axial vector meson such as $a_1, b_1, K_{1A}, K_{1B}, K_1(1270)$ and $K_1(1400)$. The branching ratio of the non-leptonic decay $B^0 \rightarrow K_1^+\pi^-$ was analyzed by using the strong coupling constants of $D_s DK_1, D_s^* DK_1$ and $D_s^* D^* K_1$ vertices for $K_1(1270)$ and $K_1(1400)$ mesons. We estimated the branching ratio values of these decays in different values of the mixing angle θ_K . Our results for the branching ratios of $B^0 \rightarrow K_1^+(1270, 1400)\pi^-$ decays were in a good agreement with the experimental values in $\theta_K = (72 \pm 3)^\circ$.

TABLE VI: Branching ratio values for $B^0 \rightarrow K_1^+(1270, 1400)\pi^-$ decays via other methods in different mixing angles in units of 10^{-5} .

Decay	$(\theta_K = 32^\circ)[42]$	$(\theta_K = 32^\circ)[43]$	$(\theta_K = -37^\circ)[44]$	$(\theta_K = -33^\circ)[45]$	$(\theta_K = -58^\circ)[45]$
$B^0 \rightarrow K_1^+(1270)\pi^-$	0.43	0.76	0.30	0.46	0.32
$B^0 \rightarrow K_1^+(1400)\pi^-$	0.23	0.40	0.54	0.30	0.45

TABLE VII: Our results for the branching ratios of $B^0 \rightarrow K_1^+(1270, 1400)\pi^-$ decays in units of 10^{-5} .

Decay	$\theta_K = 32^\circ$	$\theta_K = -37^\circ$	$\theta_K = -33^\circ$	$\theta_K = -58^\circ$
$B^0 \rightarrow K_1^+(1270)\pi^-$	4.19 ± 0.85	1.54 ± 0.56	1.41 ± 0.34	0.12 ± 0.05
$B^0 \rightarrow K_1^+(1400)\pi^-$	0.20 ± 0.02	3.42 ± 1.03	3.24 ± 0.43	3.94 ± 0.72

Appendix: Twist Function Definitions

In this appendix, we present the definitions for the two-parton distribution amplitudes as well as the twist functions. The two-parton chiral-even distribution amplitudes are given by [18]:

$$\begin{aligned}\langle 0|\bar{q}(x)\gamma_\mu\gamma_5q'(0)|A(p,\varepsilon)\rangle &= if_A m_A \int_0^1 du e^{-iup.x} \left\{ p_\mu \frac{\varepsilon.x}{p.x} \Phi_{\parallel}(u) + \left(\varepsilon_\mu - p_\mu \frac{\varepsilon.x}{p.x} \right) g_{\perp}^{(a)}(u) + \mathcal{O}(x^2) \right\}, \\ \langle 0|\bar{q}(x)\gamma_\mu q'(0)|A(p,\varepsilon)\rangle &= -if_A m_A \epsilon_{\mu\nu\rho\sigma} \varepsilon^\nu p^\rho x^\sigma \int_0^1 du e^{-iu.p.x} \left\{ \frac{g_{\perp}^{(v)}(u)}{4} + \mathcal{O}(x^2) \right\},\end{aligned}$$

also, the two-parton chiral-odd distribution amplitudes are defined by:

$$\begin{aligned}\langle 0|\bar{q}(x)\sigma_{\mu\nu}\gamma_5q'(0)|A(p,\varepsilon)\rangle &= f_A^\perp \int_0^1 du e^{-iup'.x} \left\{ (\varepsilon_\mu p_\nu - \varepsilon_\nu p_\mu) \Phi_{\perp}(u) + \frac{m_A^2 \varepsilon.x}{(p.x)^2} (p_\mu x_\nu - p_\nu x_\mu) \bar{h}_{\parallel}^{(t)} + \mathcal{O}(x^2) \right\}, \\ \langle 0|\bar{q}(x)\gamma_5q'(0)|A(p,\varepsilon)\rangle &= f_A^\perp m_A^2 (\varepsilon.x) \int_0^1 du e^{-iup.x} \left\{ \frac{h_{\parallel}^{(p)}(u)}{2} + \mathcal{O}(x^2) \right\}.\end{aligned}$$

We take into account the approximate forms of the twist-2 functions, for $A = a_1$ and K_{1A} states, to be [46]

$$\begin{aligned}\Phi_{\parallel}(u) &= 6u\bar{u} \left[1 + 3a_1^{\parallel} \xi + a_2^{\parallel} \frac{3}{2} (5\xi^2 - 1) \right], \\ \Phi_{\perp}(u) &= 6u\bar{u} \left[a_0^{\perp} + 3a_1^{\perp} \xi + a_2^{\perp} \frac{3}{2} (5\xi^2 - 1) \right],\end{aligned}$$

and for $A = b_1$ and K_{1B} to be

$$\begin{aligned}\Phi_{\parallel}(u) &= 6u\bar{u} \left[a_0^{\parallel} + 3a_1^{\parallel} \xi + a_2^{\parallel} \frac{3}{2} (5\xi^2 - 1) \right], \\ \Phi_{\perp}(u) &= 6u\bar{u} \left[1 + 3a_1^{\perp} \xi + a_2^{\perp} \frac{3}{2} (5\xi^2 - 1) \right],\end{aligned}$$

where $\xi = 2u - 1$ and $\bar{u} = 1 - u$. Also a_i^{\parallel} and a_i^{\perp} ($i = 0, 1, 2$) are defined as the Gegenbauer moments of Φ_{\parallel} and Φ_{\perp} , respectively. The values of the Gegenbauer moments for each axial vector meson are given in Ref. [18].

For the relevant two-parton twist-3 chiral-even distribution amplitudes of $A = a_1$ and K_{1A} , we take the approximate expressions up to conformal spin 9/2 and $\mathcal{O}(m_s)$ as [46]:

$$\begin{aligned}g_{\perp}^{(a)}(u) &= \frac{3}{4} (1 + \xi^2) + \frac{3}{2} a_1^{\parallel} \xi^3 + \left(\frac{3}{7} a_2^{\parallel} + 5\zeta_{3,A}^V \right) (3\xi^2 - 1) \\ &+ \left(\frac{9}{112} a_2^{\parallel} + \frac{105}{16} \zeta_{3,A}^A - \frac{15}{64} \zeta_{3,A}^V \omega_A^V \right) (35\xi^4 - 30\xi^2 + 3) \\ &+ 5 \left[\frac{21}{4} \zeta_{3,A}^V \sigma_A^V + \zeta_{3,A}^A \left(\lambda_A^A - \frac{3}{16} \sigma_A^A \right) \right] \xi (5\xi^2 - 3) \\ &- \frac{9}{2} \bar{a}_1^{\perp} \tilde{\delta}_+ \left(\frac{3}{2} + \frac{3}{2} \xi^2 + \ln u + \ln \bar{u} \right) - \frac{9}{2} \bar{a}_1^{\perp} \tilde{\delta}_- (3\xi + \ln \bar{u} - \ln u),\end{aligned}$$

$$\begin{aligned}g_{\perp}^{(v)}(u) &= 6u\bar{u} \left\{ 1 + \left(a_1^{\parallel} + \frac{20}{3} \zeta_{3,A}^A \lambda_A^A \right) \xi \right. \\ &+ \left[\frac{1}{4} a_2^{\parallel} + \frac{5}{3} \zeta_{3,A}^V \left(1 - \frac{3}{16} \omega_A^V \right) + \frac{35}{4} \zeta_{3,A}^A \right] (5\xi^2 - 1) \\ &+ \frac{35}{4} \left(\zeta_{3,A}^V \sigma_A^V - \frac{1}{28} \zeta_{3,A}^A \sigma_A^A \right) \xi (7\xi^2 - 3) \left. \right\} \\ &- 18 \bar{a}_1^{\perp} \tilde{\delta}_+ (3u\bar{u} + \bar{u} \ln \bar{u} + u \ln u) - 18 \bar{a}_1^{\perp} \tilde{\delta}_- (u\bar{u}\xi + \bar{u} \ln \bar{u} - u \ln u),\end{aligned}$$

$$\begin{aligned}
h_{\parallel}^{(t)}(u) &= 3a_0^{\perp}\xi^2 + \frac{3}{2}a_1^{\perp}\xi(3\xi^2 - 1) + \frac{3}{2}\left[a_2^{\perp}\xi + \zeta_{3,A}^{\perp}\left(5 - \frac{\omega_A^{\perp}}{2}\right)\right]\xi(5\xi^2 - 3) \\
&\quad + \frac{35}{4}\zeta_{3,A}^{\perp}\sigma_A^{\perp}(35\xi^4 - 30\xi^2 + 3) + 18\bar{a}_2^{\parallel}\left[\delta_+\xi - \frac{5}{8}\delta_-(3\xi^2 - 1)\right] \\
&\quad - \frac{3}{2}\left(\delta_+\xi[2 + \ln(\bar{u}u)] + \delta_-[1 + \xi\ln(\bar{u}/u)]\right)(1 + 6\bar{a}_2^{\parallel}),
\end{aligned}$$

$$\begin{aligned}
h_{\parallel}^{(p)}(u) &= 6u\bar{u}\left\{a_0^{\perp} + \left[a_1^{\perp} + 5\zeta_{3,A}^{\perp}\left(1 - \frac{1}{40}(7\xi^2 - 3)\omega_A^{\perp}\right)\right]\xi\right. \\
&\quad \left.+ \left(\frac{1}{4}a_2^{\perp} + \frac{35}{6}\zeta_{3,A}^{\perp}\sigma_A^{\perp}\right)(5\xi^2 - 1) - 5\bar{a}_2^{\parallel}\left[\delta_+\xi + \frac{3}{2}\delta_-(1 - \bar{u}u)\right]\right\} \\
&\quad - 3[\delta_+(\bar{u}\ln\bar{u} - u\ln u) + \delta_-(u\bar{u} + \bar{u}\ln\bar{u} + u\ln u)](1 + 6\bar{a}_2^{\parallel}),
\end{aligned}$$

where

$$\tilde{\delta}_{\pm} = \frac{f_A^{\perp} m_{q_2} \pm m_{q_1}}{f_A m_A}, \quad \zeta_{3,A}^{V(A)} = \frac{f_{3A}^{V(A)}}{f_A m_A}.$$

In these phrases, the values of all parameters such as ω_A^V , σ_A^{\perp} and etc. are given in Ref. [18] for each meson. On the other hand, the same as the above quantities but for $A = b_1$ and K_{1B} states are given as follows.

$$\begin{aligned}
g_{\perp}^{(a)}(u) &= \frac{3}{4}a_0^{\parallel}(1 + \xi^2) + \frac{3}{2}a_1^{\parallel}\xi^3 + 5\left[\frac{21}{4}\zeta_{3,A}^V + \zeta_{3,A}^A\left(1 - \frac{3}{16}\omega_A^A\right)\right]\xi(5\xi^2 - 3) \\
&\quad + \frac{3}{16}a_2^{\parallel}(15\xi^4 - 6\xi^2 - 1) + 5\zeta_{3,A}^V\lambda_A^V(3\xi^2 - 1) \\
&\quad + \frac{105}{16}\left(\zeta_{3,A}^A\sigma_A^A - \frac{1}{28}\zeta_A^V\sigma_A^V\right)(35\xi^4 - 30\xi^2 + 3) \\
&\quad - 15\bar{a}_2^{\perp}\left[\tilde{\delta}_+\xi^3 + \frac{1}{2}\tilde{\delta}_-(3\xi^2 - 1)\right] \\
&\quad - \frac{3}{2}\left[\tilde{\delta}_+(2\xi + \ln\bar{u} - \ln u) + \tilde{\delta}_-(2 + \ln u + \ln\bar{u})\right](1 + 6\bar{a}_2^{\perp}),
\end{aligned}$$

$$\begin{aligned}
g_{\perp}^{(v)}(u) &= 6u\bar{u}\left\{a_0^{\parallel} + a_1^{\parallel}\xi + \left[\frac{1}{4}a_2^{\parallel} + \frac{5}{3}\zeta_{3,A}^V\left(\lambda_A^V - \frac{3}{16}\sigma_A^V\right) + \frac{35}{4}\zeta_{3,A}^A\sigma_A^A\right](5\xi^2 - 1)\right. \\
&\quad \left.+ \frac{20}{3}\xi\left[\zeta_{3,A}^A + \frac{21}{16}\left(\zeta_{3,A}^V - \frac{1}{28}\zeta_{3,A}^A\omega_A^A\right)(7\xi^2 - 3)\right]\right. \\
&\quad \left.- 5\bar{a}_2^{\perp}[2\tilde{\delta}_+\xi + \tilde{\delta}_-(1 + \xi^2)]\right\} \\
&\quad - 6\left[\tilde{\delta}_+(\bar{u}\ln\bar{u} - u\ln u) + \tilde{\delta}_-(2u\bar{u} + \bar{u}\ln\bar{u} + u\ln u)\right](1 + 6\bar{a}_2^{\perp}),
\end{aligned}$$

$$\begin{aligned}
h_{\parallel}^{(t)}(u) &= 3\xi^2 + \frac{3}{2}a_1^{\perp}\xi(3\xi^2 - 1) + \left[\frac{3}{2}a_2^{\perp}\xi + \frac{15}{2}\zeta_{3,A}^{\perp}\left(\lambda_A^{\perp} - \frac{1}{10}\sigma_A^{\perp}\right)\right]\xi(5\xi^2 - 3) \\
&\quad + \frac{35}{4}\zeta_{3,A}^{\perp}(35\xi^4 - 30\xi^2 + 3) \\
&\quad + \frac{9}{2}\bar{a}_1^{\parallel}\xi\left[\delta_+(\ln u - \ln\bar{u} - 3\xi) - \delta_-\left(\ln u + \ln\bar{u} + \frac{8}{3}\right)\right],
\end{aligned}$$

$$\begin{aligned}
h_{\parallel}^{(p)}(u) = & 6u\bar{u} \left\{ 1 + a_1^{\perp} \xi + \left(\frac{1}{4} a_2^{\perp} + \frac{35}{6} \zeta_{3,A}^{\perp} \right) (5\xi^2 - 1) \right. \\
& \left. + 5\zeta_{3,A}^{\perp} \left[\lambda_A^{\perp} - \frac{1}{40} (7\xi^3 - 3)\sigma_A^{\perp} \right] \xi \right\} \\
& - 9\bar{a}_1^{\parallel} \delta_+ (3u\bar{u} + \bar{u} \ln \bar{u} + u \ln u) - 9\bar{a}_1^{\parallel} \delta_- \left(\frac{2}{3} \xi u\bar{u} + \bar{u} \ln \bar{u} - u \ln u \right).
\end{aligned}$$

-
- [1] R. Casalbuoni, A. Deandrea, N. Di Bartolomeo, R. Gatto, F. Feruglio, and G. Nardulli, Phys. Rept. **281**, 145 (1997).
- [2] M. E. Bracco, M. Chiapparini, F. S. Navarra, and M. Nielsen, Phys. Lett. B **659**, 559 (2008).
- [3] F. S. Navarra, M. Nielsen, M. E. Bracco, M. Chiapparini, and C. L. Schat, Phys. Lett. B **489**, 319 (2000).
- [4] F. S. Navarra, M. Nielsen, and M. E. Bracco, Phys. Rev. D **65**, 037502 (2002).
- [5] M. E. Bracco, M. Chiapparini, A. Lozea, F. S. Navarra, and M. Nielsen, Phys. Lett. B **521**, 1 (2001).
- [6] B. O. Rodrigues, M. E. Bracco, M. Nielsen, and F. S. Navarra, Nucl. Phys. A **852**, 127 (2011).
- [7] R. D. Matheus, F. S. Navarra, M. Nielsen, and R. R. da Silva, Phys. Lett. B **541**, 265 (2002).
- [8] R. R. da Silva, R. D. Matheus, F. S. Navarra, and M. Nielsen, Braz. J. Phys. **34**, 236 (2004).
- [9] Z. G. Wang, and S. L. Wan, Phys. Rev. D **74**, 014017 (2006).
- [10] Z. G. Wang, Nucl. Phys. A **796**, 61 (2007).
- [11] F. Carvalho, F. O. Duraes, F. S. Navarra, and M. Nielsen, Phys. Rev. C **72**, 024902 (2005).
- [12] M. E. Bracco, A. J. Cerqueira, M. Chiapparini, A. Lozea, and M. Nielsen, Phys. Lett. B **641**, 286 (2006).
- [13] L. B. Holanda, R. S. Marques de Carvalho, and A. Mihara, Phys. Lett. B **644**, 232 (2007).
- [14] R. Khosravi, and M. Janbazi, Phys. Rev. D **87**, 016003 (2013).
- [15] R. Khosravi, and M. Janbazi, Phys. Rev. D **89**, 016001 (2014).
- [16] M. Janbazi, N. Ghahramany, and E. Pourjafarabadi, Eur. Phys. J. C **74**, 2718 (2014).
- [17] T. Huang, Z. H. Li and F. Zuo, Eur. Phys. J. C **60**, 63 (2009).
- [18] K. Yang, Phys. Rev. D **78**, 034018 (2008).
- [19] A. Hayashigaki and K. Terasaki, arXiv: 0411285 [hep-ph].
- [20] M. Tanabashi et al. (Particle Data Group), Phys. Rev. D **98**, 030001 (2018).
- [21] P. Gelhausen, A. Khodjamirian, A. A. Pivovarov and D. Rosenthal, Phys. Rev. D **88**, 014015 (2014).
- [22] Z. GangWang, Eur. Phys. J. C **52**, 553560 (2007).
- [23] M. E. Bracco, M. Chiapparini, F. S. Navarra and M. Nielsen, Phys. Lett. B **659**, 559 (2008).
- [24] L. Burakovsky and T. Goldman, Phys. Rev. D **57**, 2879 (1998).
- [25] M. Suzuki, Phys. Rev. D **47**, 1252 (1993).
- [26] H. Y. Cheng, Phys. Rev. D **67**, 094007 (2003).
- [27] H. Hatanaka, K. C. Yang, Phys. Rev. D **77**, 094023 (2008).
- [28] A. Tayduganov, E. Kou, and A. Le Yaouanc, Phys. Rev. D **85**, 074011 (2012).
- [29] F. Divotgey, L. Olbrich and F. Giacosa, Eur. Phys. J. A **49**, 135 (2103).
- [30] B. Aubert, et al., BABAR Collaboration, Phys. Rev. D **81**, 052009 (2010).
- [31] C. Isola, M. Ladisa, G. Nardulli, and P. Santorelli, Phys. Rev. D **68**, 114001 (2003).
- [32] C. Isola, M. Ladisa, G. Nardulli, T. N. Pham, and P. Santorelli, Phys. Rev. D **64**, 014029 (2001).
- [33] R. Fleischer, Z. Phys. C **58**, 483 (1993).
- [34] R. Fleischer, Z. Phys. C **62**, 81 (1994).
- [35] M. Ciuchini, E. Franco, G. Martinelli, L. Reina, and L. Silvestrini, Phys. Lett. B **316**, 127 (1993).
- [36] M. Ciuchini, E. Franco, G. Martinelli, and L. Reina, Nucl. Phys. B **415**, 403 (1994).
- [37] A. J. Buras, in Probing the Standard Model of Particle Interactions (Elsevier Science B. V., 1998), arXiv: 9806471 [hep-ph].
- [38] R. Casalbuoni, A. Deandrea, N. Di Bartolomeo, F. Feruglio, R. Gatto, and G. Nardulli, Phys. Rept. **281**, 145 (1997).
- [39] M. Bando, T. Kugo, and K. Yamawaki, Phys. Rept. **164**, 217 (1988).
- [40] S. Ahmed et al., CLEO Collaboration, Phys. Rev. Lett. **87**, 251501 (2001).
- [41] A. Ali and C. Greub, Phys. Rev. D **57**, 2996 (1998).
- [42] G. Calderon, J. H. Canoz, and C. E. Vera, Phys. Rev. D **76**, 094019 (2007).
- [43] V. Laporta, G. Nardulli, and T. N. Pham, Phys. Rev. D **74**, 054035 (2006).
- [44] H. Y. Cheng and K. C. Yang, Phys. Rev. D **76**, 114020, (2007).
- [45] Z. Q. Zhang, Z. W. Hou, Y. Yang, and J. Sun, Phys. Rev. D **90**, 074023 (2014).
- [46] K. Yang, Nucl. Phys. B **776**, 187 (2007).